frontiers | Frontiers in Built Environment

TYPE Original Research
PUBLISHED 09 May 2024
DOI 10.3389/fbuil.2024.1403460

OPEN ACCESS

EDITED BY
Paul Awoyera,
Covenant University, Nigeria

REVIEWED BY
Afaq Ahmad,
University of Engineering and Technology, Pakistan
Panagiotis G. Asteris,
School of Pedagogical and Technological Education, Greece

*CORRESPONDENCE
Mary Subaja Christo,
marysubaja@gmail.com
Kennedy Onyelowe,
konyelowe@mouau.edu.ng
Sathvik S.,
sathvik-cvl@dayanandasagar.edu

RECEIVED 19 March 2024
ACCEPTED 22 April 2024
PUBLISHED 09 May 2024

CITATION
George C, Zumba E, Procel Silva MA, Selvan SS, Christo MS, Kumar R, Kumar Singh A, S. S and Onyelowe K (2024), Predicting the fire-induced structural performance of steel tube columns filled with SFRC-enhanced concrete: using artificial neural networks approach.
Front. Built Environ. 10:1403460.
doi: 10.3389/fbuil.2024.1403460

Predicting the fire-induced structural performance of steel tube columns filled with SFRC-enhanced concrete: using artificial neural networks approach

Christo George[1], Edwin Zumba[2,3], Maria Alexandra Procel Silva[4], S. Senthil Selvan[1], Mary Subaja Christo[5]*, Rakesh Kumar[6], Atul Kumar Singh[7], Sathvik S.[7]* and Kennedy Onyelowe[8]*

[1]Department of Civil Engineering, College of Engineering and Technology, SRM Institute of Science and Technology, Chennai, India, [2]Universidad Nacional de Chimborazo (UNACH), Riobamba, Ecuador, [3]Universidad Politecnica de Madrid (UPM), Madrid, Spain, [4]Facultad de Administracion de Empresas, Escuela Superior Politecnica de Chimborazo (ESPOCH), Riobamba, Ecuador, [5]Department of Networking and Communications, School of Computing, SRM Institute of Science and Technology, Chennai, India, [6]Department of Civil Engineering, National Institute of Technology, Patna, India, [7]Department of Civil Engineering, Dayananda Sagar College of Engineering, Bangalore, India, [8]Department of Civil Engineering, Michael Okpara University of Agriculture, Umudike, Nigeria

Predicting the axial Shortening strength of concrete-filled steel tubular (CFST) columns is an important problem that this study attempts to solve for civil engineering projects. We suggest using a deep learning-based artificial neural network (ANN) model to address this issue, taking into account the intricate relationship between steel tube and core concrete. The model, called ANN-SFRC (Steel Fibre Reinforced Concrete), surpasses an R^2 threshold of 0.90 and achieves impressive R^2 values across different types of CFST columns. Compared to traditional linear regression methods, the ANN-SFRC model significantly improves accuracy, with an observed inaccuracy of less than 3% compared to actual values. With its reliable approach to forecasting the behavior of CFST columns under axial compression, this high-performance instrument enhances safety and accuracy during the design and planning stages of civil engineering.

KEYWORDS

structural performance, steel fibre reinforced concrete, concrete filled steel tube, ANN, ambient and elevated temperatures

1 Introduction

Concrete is poured into steel-tube columns (CFST) to increase the engineering constructions' toughness (strength and ductility). This method is called a "composite system," which blends concrete with other composite materials (Chandramouli et al., 2022; Fischer et al., 2022; Mohammed et al., 2023; Đorđević and Kostić, 2023). A CFST member is typically made by filling a hollow steel tube with concrete. The main advantage of employing steel tubes filled with concrete as the main component is that it considerably increases the

toughness and plasticity of the concrete while also delaying or preventing local steel tubular buckling (George and Selvan, 2024).

The characteristics that make CFST unique include toughness, more remarkable plasticity, increased bearing capacity, improved seismic performance, and practical construction refractory capabilities. Additionally, CFST is used as a 'structure' in buildings in various shapes (such as circular, square, and rectangle) depending on the environment and the sectional form needs. Since square CFSTs are easier to process and more stable than other shapes [6–8], more investigations have focused on them than rectangular and circular tubes. The main reasons for the increased use of CFST members are the steel tube's improved tensile strength and the concrete core's compressive strength.

Although the square, rectangular, and circular (Singh et al., 2023), octagonal, round-ended rectangle, and square, rectangular, and circular-based models (Liao et al., 2021) are the three main varieties of CFST, there are many other shapes. They are not the only shapes that can be used. Similar divisions of the CFST into confined and unconfined cross-sectional forms exist. To predict material properties like yield strength, compressive strength, ultimate bearing capacity, ductility, thickness, and others, each CFST form employs a unique parametric model. To correctly forecast or approximate the CFST and its axial compression capacity and to evaluate them, empirical formulas must be used (Romero et al., 2011).

Concrete-filled steel tube columns have gained widespread attention in structural engineering due to their remarkable structural performance and versatility. These columns, composed of a steel tube filled with high-strength concrete, exhibit enhanced strength, ductility, and fire resistance compared to traditional structural elements. Despite their increasing use, a comprehensive understanding of the system parameters influencing CFST column performance is crucial for optimal design and application.

The literature review indicates that only a few studies have investigated the behaviour of CFST columns filled with Steel Fibre Reinforced Concrete (SFRC) under elevated temperatures. Meng et al. (Ujwal et al., 2024) conducted fire resistance experiments on eight CFST columns filled with steel fiber, highlighting a notable enhancement in fire performance, especially in an inner steel profile. Columns exposed to fire on one or two sides exhibited fire durations exceeding 240 min. A study addressing the long-term shrinkage of concrete (Sharma et al., 2022; Sathvik et al., 2023) emphasized its significant impact on strength, attributing this effect to the gradual evaporation of water and its impact on the efficiency of wet particle packing. (George et al., 2024). observed that using steel fibers in self-stressing concrete-filled steel tube columns could improve the bending moment by 2%–14% and increase the maximum load by 4%–17%. Although the increase is subtle, steel fibers delay secondary actions, demonstrating an increased bending moment after reaching ultimate conditions, indicating a satisfactory margin for error. Song et al. (Moliner et al., 2013) explored CFST series with expansive and regular concrete, subjecting them to temperatures ranging from 20°C to 800°C to examine the temperature's effect on bond behavior. The results revealed a 98% reduction in bond capacity after heating to 800°C, primarily due to diminishing contributions from factors such as chemical adhesion at high temperatures. Studies by Romero et al. [17] and Moliner et al. (Song et al., 2017) investigated the impact of steel fibers on fire resistance, showing that the addition of mixed steel fibers increased fire resistance in columns—a conclusion supported by other studies (Han et al., 2018; Murali and Azab, 2023). Despite ample literature on the structural behaviour of CFST filled with standard concrete, the influence of SFRC in CSFT remains relatively unexplored, underscoring the necessity for further research in this domain.

Since the datasets are metadata and different calculations, the researchers have chosen to analyze the axial compression capacity (A.C.C.) kinds using CFST 'Machine Learning' based methods. Even while "expected errors" or "loss percentage rate" are technically "expected errors" in the assessment of datasets to recover the expected results, machine learning is still regarded as a computerized language/computation and standardized technique (Zhou and Liu, 2019; Wróblewska and Kowalski, 2020). Due to the wealth of information and understanding of the CFST column members, not many countries support this strategy. However, because CFST-based bridges have a far higher threshold capacity than conventional concrete-based columns, nations like Japan, China, the US, India, and others have chosen them as a priority method in structural engineering. Even if only a small number of CFST experiments were successful, it is feasible that they could falter under pressure and have consequences in real time because of changes and variations in the environment (Raja et al., 2021; Zarringol and Thai, 2022). Despite being successful as prototypes, new models developed by researchers have also failed (Le et al., 2021). Therefore, environmental or external elements should be considered before beginning projects for buildings and bridges that use CFST-based columns.

China hurriedly constructed over 413 CFST bridges in 2015, each with a 50-meter span (Asteris et al., 2021). They formed highly ductile, ultimately load-bearing based columns using the knowledge they received during the testing phases on circular and rectangular CFSTs and used them in their projects. The CFST columns-based structural strength is more suited for bridges because of its capacity to manage external challenges, including heavy vehicle load, wind, erosion, ductility, toughness, and elastoplastic properties (Han et al., 2005).

The application of Machine Learning (ML) and Deep Learning (DL) techniques for predicting and modeling the behavior of concrete and Fiber-Reinforced Concrete (FRC) at elevated temperatures. It highlights the advantages of employing ML/DL models, such as their efficiency in estimating material behaviors under fire conditions, offering insightful research ideas, and presenting future scope for researchers and engineers globally. ML/DL models demonstrate significant advantages over traditional experimental testing and numerical tools, particularly in their ability to handle high nonlinearity associated with concrete/FRC behavior at elevated temperatures. These models offer simplicity in mathematical paradigms, time efficiency, and a wide range of modeling options. They also reduce dependency on commercial software and conserve limited experimental resources. Despite the promising performance of ML/DL algorithms in predicting concrete/FRC properties under high temperatures, significant research gaps persist. Further studies are needed to predict mechanical and other physical properties accurately. Existing ML/DL models for this purpose are still premature and require refinement for practical applications. Additionally, challenges related to data extraction, preprocessing,

dataset preparation, feature selection, and model training and validation need to be addressed. (46).

2 Research significance

Concrete-filled steel tubular (CFST) columns play a crucial role in the structural integrity of civil engineering projects. The axial shortening strength of CFST columns is a paramount concern, and precise prediction of this strength is vital for ensuring the safety and efficiency of such projects. However, a significant research gap exists in developing high-performance predictive models for CFST columns. The evaluation of the literature highlights important knowledge gaps regarding the behavior of concrete-filled steel tubular (CFST) columns under high temperatures and the effects of long-term shrinkage, especially those filled with steel fibre reinforced concrete (SFRC). Even though steel fibers have shown encouraging results in improving structural performance and fire resistance, thorough studies in these particular fields are still lacking. Furthermore, the lack of machine learning-based predictive models for the performance of CFST columns and the scant investigation of the influence of environmental factors point to important directions for future study. By filling in these gaps and investigating applications like improving predictive modeling, validating experiments, developing design guidelines, and putting them into practice, we can greatly increase the resilience, efficiency, and safety of CFST-based structures in civil engineering projects. Thus, the current study addresses this gap by applying deep learning techniques to create an Artificial Neural Network (ANN) model, specifically the ANN-SFRC model, tailored to predict the axial shortening strength of CFST columns. The intricate relationship between core concrete and steel tube properties, coupled with the nonlinearity inherent in compression behaviour, makes this research essential in enhancing the reliability of CFST column designs.

In the context of using Artificial Neural Networks (ANNs) for analyzing structural behavior the scope of the study are as follows Past Scope: Early Adoption: ANNs have been used in structural analysis for several decades, primarily in the latter half of the 20th century. Early studies focused on basic structural analysis tasks, such as static and dynamic load analysis, with relatively simple network architectures and datasets. Challenges in the past included limited computing power, lack of standardized methodologies, and relatively small datasets, which constrained the accuracy and applicability of ANN models.

Present Scope: Advanced Applications: Present-day applications of ANNs in structural analysis encompass a wide range of tasks, including predicting material properties, structural health monitoring, and optimizing structural designs. Modern ANN models feature more complex architectures, including deep learning techniques such as Convolutional Neural Networks (CNNs) and Recurrent Neural Networks (RNNs), allowing for more accurate and nuanced analyses. Availability of large-scale datasets, coupled with advances in computing power and data processing techniques, enables more comprehensive training and validation of ANN models. Validation Techniques: Present studies employ rigorous validation techniques, such as cross-validation and regularization methods, to ensure the generalization and reliability of ANN models.

Future Scope: Further Advancements: Future research in the field is expected to focus on refining ANN architectures, optimizing training algorithms, and integrating hybrid modeling approaches for enhanced accuracy and efficiency. Integration with IoT and Big Data: Integration of ANNs with Internet of Things (IoT) devices and utilization of big data analytics are anticipated to revolutionize structural analysis, enabling real-time monitoring and predictive maintenance of structures. ANNs will likely find broader applications in interdisciplinary fields such as civil engineering, architecture, and materials science, leading to more holistic and sustainable approaches to structural design and analysis.

The present study likely employs more advanced ANN architectures and techniques compared to previous studies, leading to improved accuracy and robustness in predicting structural behavior. With access to larger and more diverse datasets, the present study benefits from better data quality and increased representativeness of real-world scenarios. Validation processes, as discussed in the provided conclusion, ensure that the ANN models developed in the present study exhibit superior generalization ability and effectiveness compared to earlier studies.

3 Materials and methods

3.1 Properties of materials

Rectangular sections were used to construct the CFST column tensile test in ASTM-E8/8 M in line with the code (Liew et al., 2016). The characteristics of steel tubes identified by sample evaluation are listed in Table 1 (which shows the mean findings of three specimens for each tube form). The study aimed to ascertain the maximum weight that could be supported by concrete columns enclosed in rectangular steel tubes. The fill was made of steel fibre reinforced concrete (SFRC), grade M30. The experiment shown in Table 1 above investigated specimens that had undergone axial shortening.

3.2 Preparation of specimen

The fundamental components of a Concrete-Filled Steel Tubular (CFST) typically consist of a concrete core encased within an iron pipe. While concrete and iron pipe are the primary constituents, additional elements may include hollow steel tubes, moisture, super softeners, or other alloying elements, depending on the specific requirements of the structural application. Notably, rectangular Concrete-Filled Steel Tube Structural Columns (CFST-SCs) are often constructed using concrete with average strength characteristics. When exposed to elevated temperatures, CFSTs made from the aforementioned concretes exhibit enhanced physical and mechanical properties (Han et al., 2007; Sarkar et al., 2023). This phenomenon is particularly advantageous, as it contributes to the improved performance of CFST columns under challenging conditions. The strengthened concrete used in these structures plays a pivotal role in augmenting key attributes of the CFST column, such as stiffness, stress capacity, and current capacities. The interaction between the concrete core and the surrounding steel tube creates a synergistic effect, combining the compressive strength of concrete with steel's ductility and tensile

TABLE 1 Material properties of rectangular steel tubes and steel fiber.

Material properties	Rectangular steel tubes	Steel fiber
Size (mm)	Size = 100 × 50 mm	L = 30 mm&D = 0.50 mm
Yield Strength f_y (MPa)	445	1,101
Ultimate strength f_u (MPa)	488	1,604
Elongation (%)	15.2	22.2
Poisson's ratio	0.28	0.27
Modulus of Elasticity E_s (GPa)	205.8	210.64

TABLE 2 Mix proportions.

Grade of concrete	Cement	Fine aggregate	Coarse aggregate	Water/Cement
M30	1	1.69	3.12	0.44

FIGURE 1
CFST Light Gauge Steel Rectangular Column test specimens.

strength. This results in a composite material with superior structural performance, making CFST columns a preferred choice in various engineering applications.

3.3 Preparation of concrete

The study used 53-grade Ordinary Portland Cement (OPC), which has a higher compressive strength than other types of OPC. (Meng et al., 2020). The cement's specific gravity of 3.15 exposes its density, while the loss of ignition value of 0.98 indicates how much volatile material is lost when heated. The fine sand can flow through the sieve's 4.75 mm opening. While a higher value indicates a coarser particle size dispersion in the sand, a lower value of the fineness modulus predicts a smaller particle size distribution (Hu et al., 2003; Sakino et al., 2004). Sand's density in terms of water is shown by its specific gravity of 2.71. Better mechanical properties are suggested by the cement's chemical composition, which contains an argillaceous proportion of approximately 30% and a neoplastic section of around 70% (Du et al., 2016). The mix proportions for various concrete grades are listed in Table 2.

The study's coarse aggregate is a well-graded, angular granite stone with a maximum size of 20 mm (Sathvik et al., 2019a). It meets the requirements of I.S.: 383–2016 (Sathvik et al., 2019b). Figure 1 shows the CFST Light gauge steel rectangular column test specimens.

3.4 Experimental techniques of steel tube

The study's principal goal, to evaluate how steel fibre reinforced concrete (SFRC)-filled concrete-filled steel tube (CFST) columns

10.3389/fbuil.2024.1403460

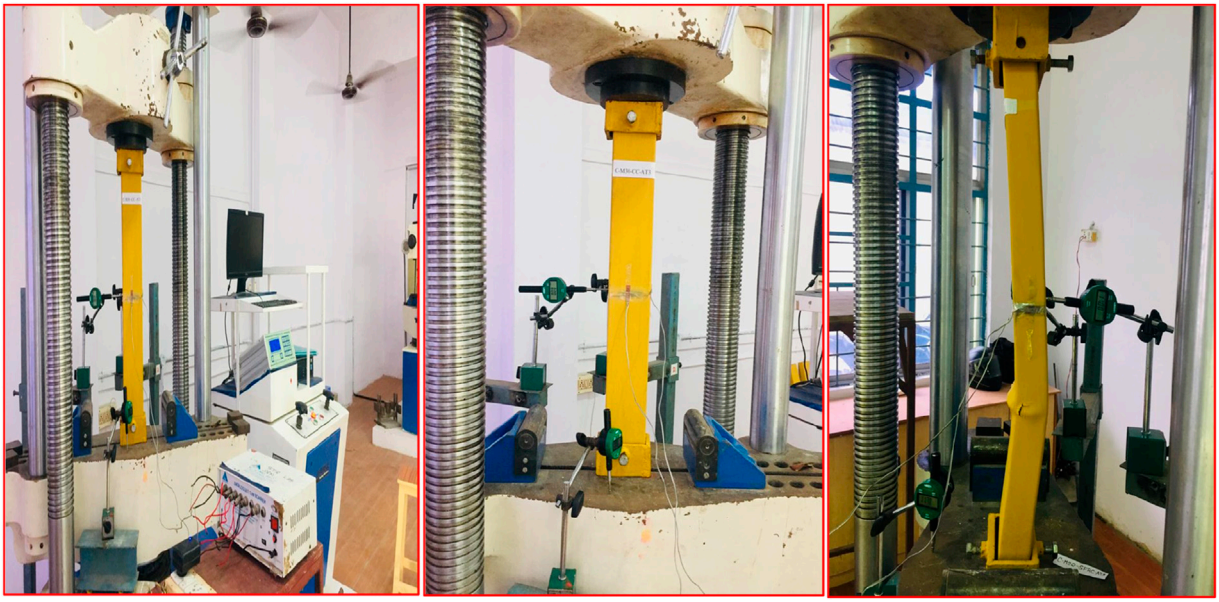

FIGURE 2
Experimental test setup.

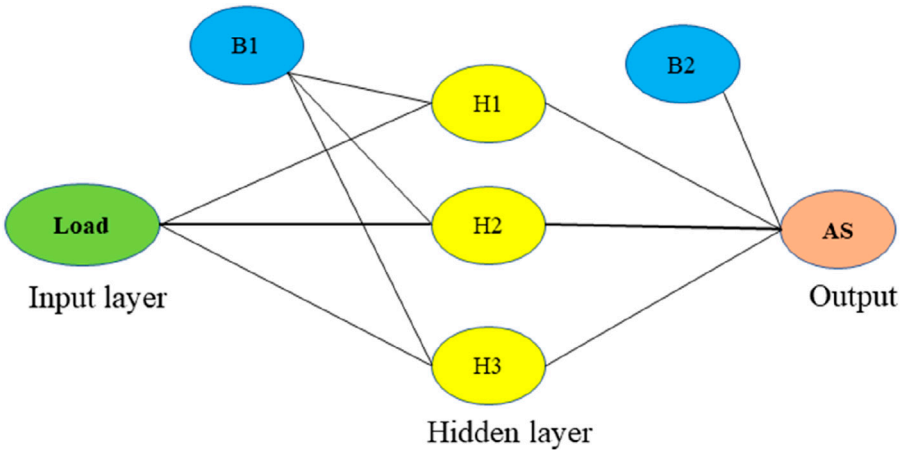

FIGURE 3
Typical structure of an ANN.

TABLE 3 Descriptive statistics of the input and output parameter.

	Mean	Median	Standard deviation	Minimum	Maximum
Load	100	100	59.89574	0	200
AS M30 CC	1.7663	1.71	0.94563935	0	3.32
AS M30 SFRC	2.41536	2.34	1.26425	0	4.56
M30 CC ELE	3.57	3.5	1.866755	0	6.75
M30 SFRC ELE	4.6297	4.2	2.331415	0	8.94

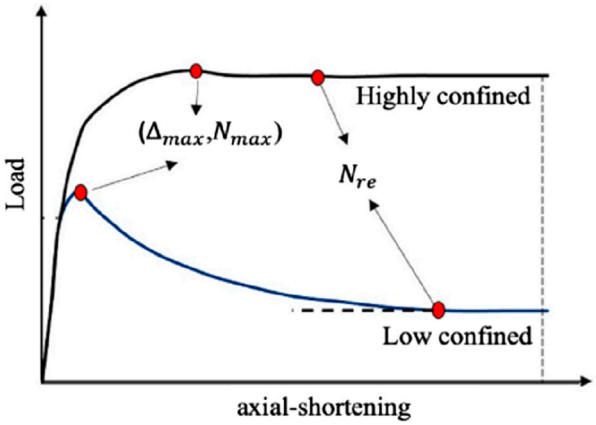

FIGURE 4
Axial load-shortening curve.

react in both average and high temperatures, is depicted in Figure 2. According to I.S.: 10262–2019, the study employs the grade of concrete (M30) with 1% steel fibre added. To make the new concrete, add coarse and fine aggregate to the mixer and mix for 2 minutes.

4 Artificial neural network

In the context of our study, we adopt the well-established information processing model known as an Artificial Neural Network (ANN), as illustrated in Figure 3. This model comprises interconnected clusters of neurons organized into input, hidden, and output layers (Ivakhnenko, 1971). The strength of ANNs lies in their ability to excel in prediction tasks by deciphering the relationships between inputs and outputs. While the literature extensively covers the structure and functionality of ANNs, our focus diverges from these topics. Our study intentionally steers clear of delving into the intricacies of ANN structure and activity, as these aspects have been thoroughly explored in existing literature. Instead, we focus on a more specific application, emphasizing our unique approach to predict the axial load-shortening curve of concentrically loaded rectangular and circular Concrete-Filled Steel Tube (CFST) columns.

Despite the immense potential of ANNs in engineering applications, previous studies often employed them merely to estimate final strength values. In contrast, our research takes an innovative approach by introducing a unique methodology specifically designed to predict the axial load-shortening behaviour of CFST columns under concentric loads. The subsequent subsection elucidates the intricacies of our approach, shedding light on the innovative techniques employed to enhance the accuracy and applicability of our predictions.

5 Result and discussion

5.1 Development of the ANN model

In Figure 4, the load-deflection curve exhibits two distinct branches: ascending and descending. Key parameters on this curve include the peak load (Nmax) and the corresponding axial shortening (max), while Nre denotes the residual strength. We aim to employ Artificial Neural Network (ANN) techniques to anticipate

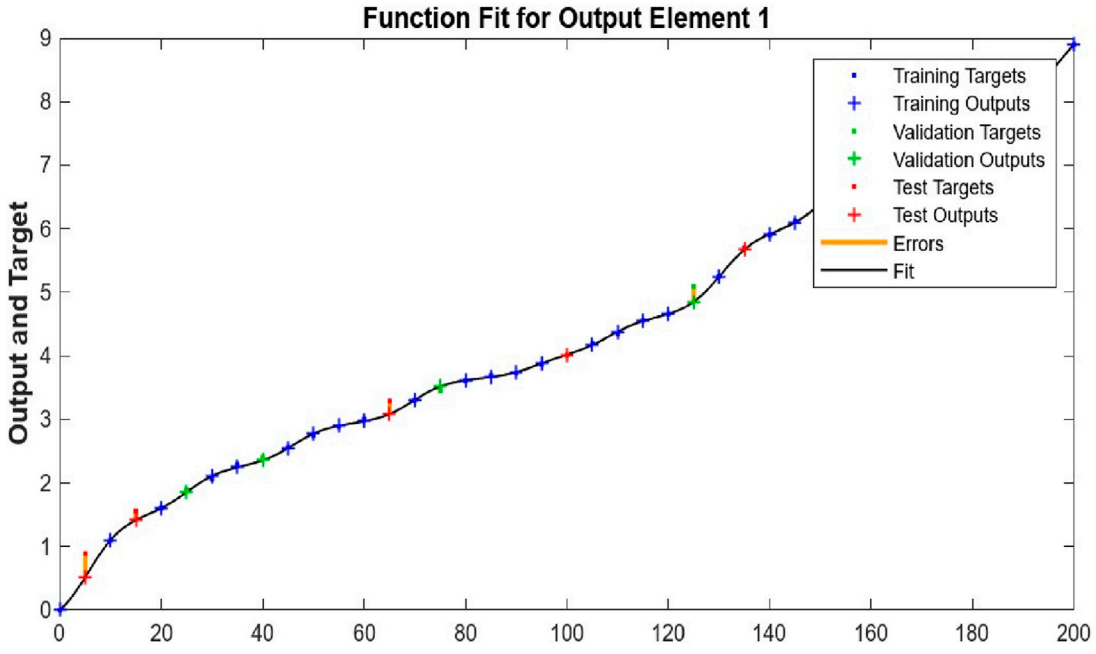

FIGURE 5
Comparing the target and predicted values.

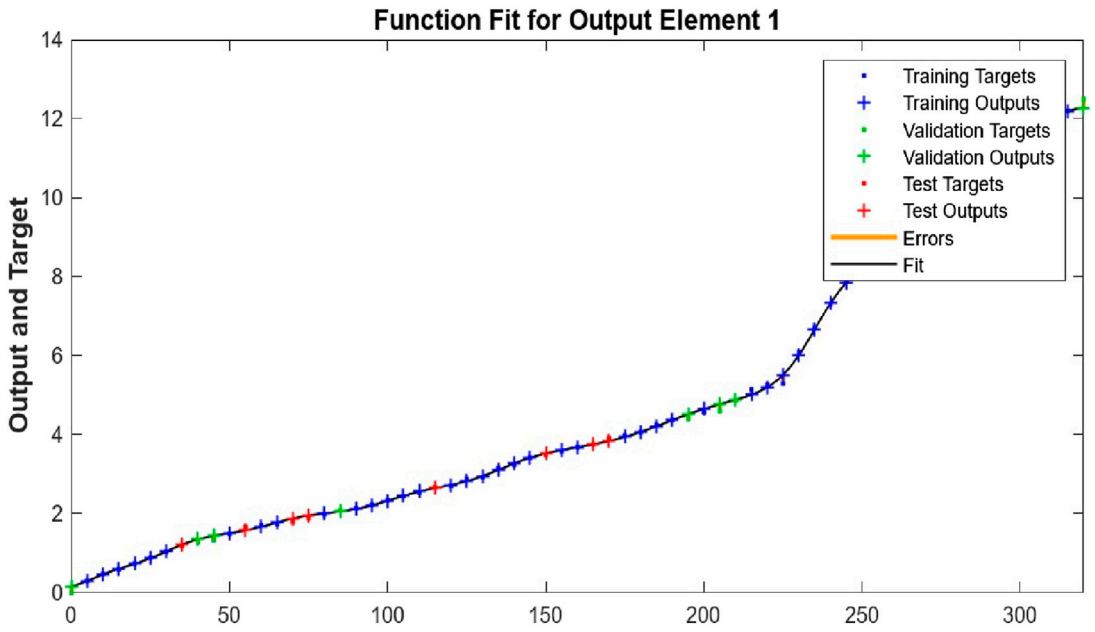

FIGURE 6
Output of the ANN model.

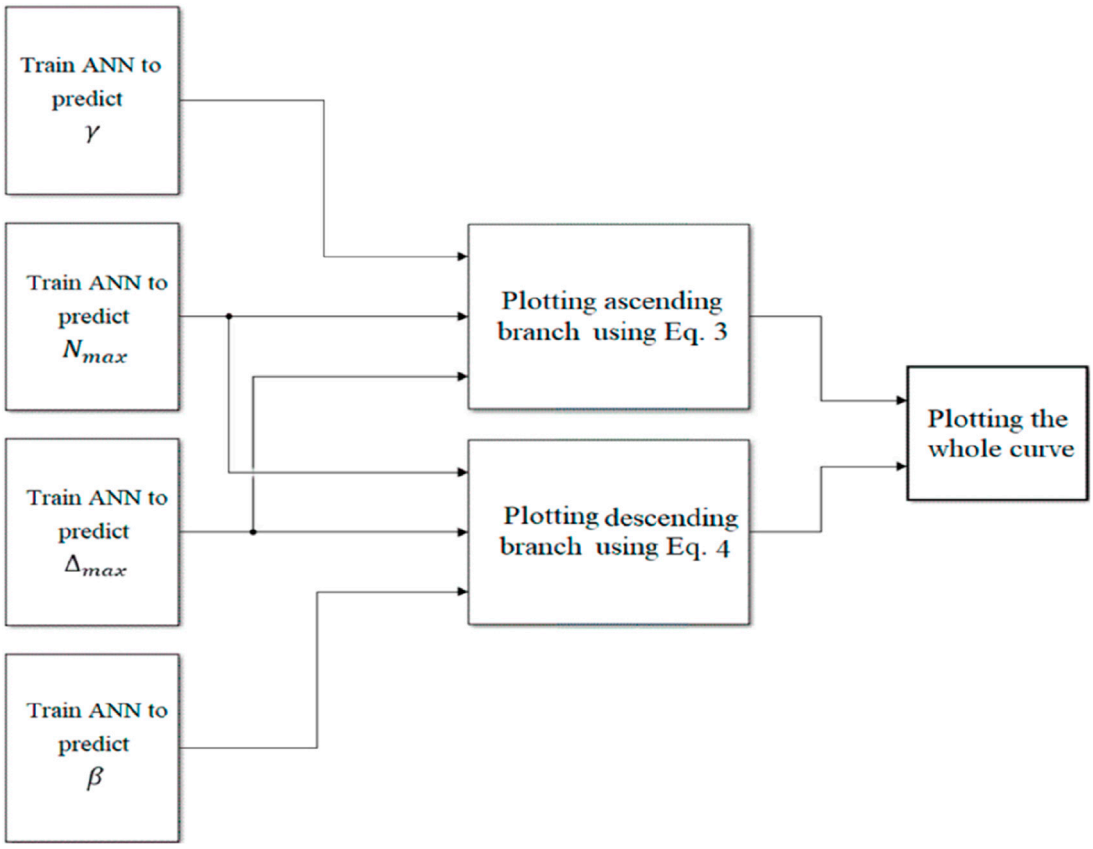

FIGURE 7
Flow diagram for the ANN-Based shortening curve Plotting approach.

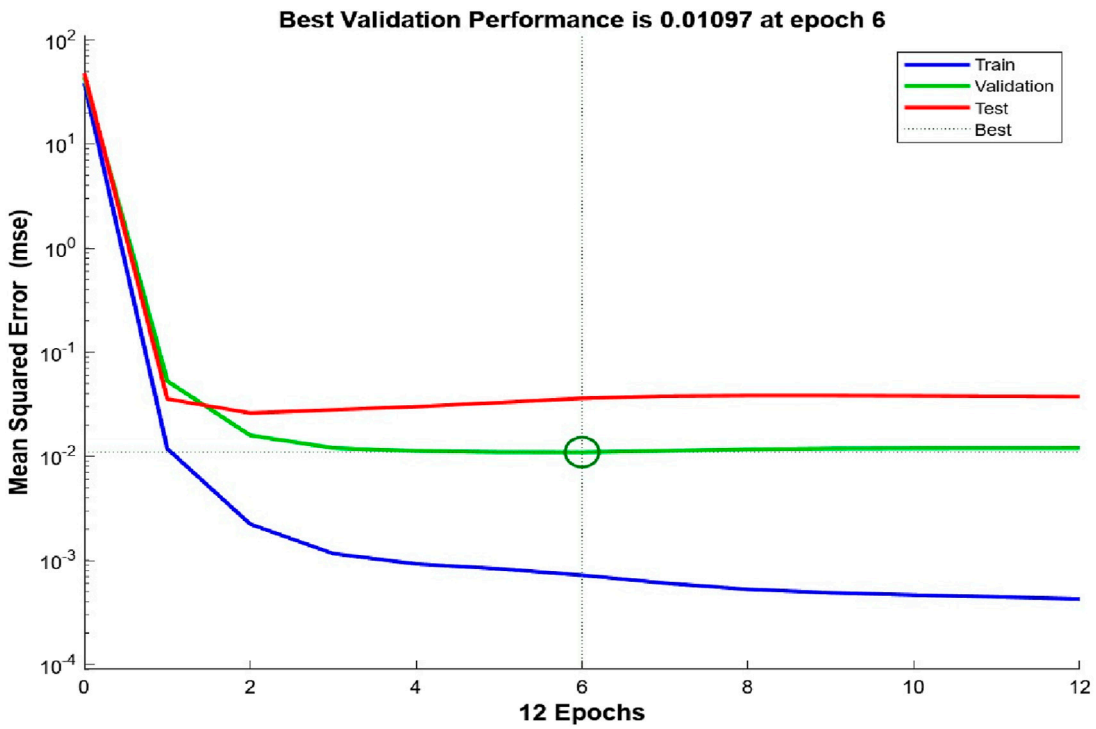

FIGURE 8
ANN models' error range (E.R.).

the load-shortening response of Concrete-Filled Steel Tube (CFST) columns. To achieve this, we constructed eight ANN models utilizing the Batch Replacement (B.R.) training approach and MATLAB's feed-forward backpropagation network. These models comprise four variations for circular and four for rectangular CFST column sections.

Creating models to predict Nmax, max, the trend of the ascending branch, and the trend of the descending branch are all part of the forecasting process. Many strategies were used to prevent the developed ANN model from overfitting. To guarantee the model's performance evaluation on untested data, the dataset was first divided into training, validation, and testing sets. The network's generalizability was then improved during the training phase by using regularization techniques like dropout to keep it from becoming unduly dependent on particular features or nodes. To reduce the possibility of overtraining, the training procedure also included early stopping criteria that were used to stop training when the model's performance on the validation set declined. To avoid overtraining, the maximum number of iterations (epochs) for all ANN models in this study was set at 90.

A total of 41 data with input feature as load have been employed as a final dataset to construct the four ANN models predict the load-shortening behavior of CFST columns. The input variables for each model includes load and ouput variable include the corresponding axial shortening for different conditions. The descriptive statistics of input and output parameters is given in Table 3. A trial-and-error tuning strategy was utilized to determine the hyperparameters, architectures, and functions of the models during the training phase. The model with the highest average prediction accuracy throughout the whole training set was selected based on these findings. The three hidden layers and one output layer comprising the optimal structure for all four ANN models. All optimal ANN were most suited for Tansig and Purelin's suitable activation functions. These models were designed to enhance the accuracy of predicting the load-shortening behavior of CFST columns, considering various geometric and material parameters in their training and evaluation processes. The dataset was subjected to multiple rounds of preprocessing prior to the development prediction models. Part of this process involved randomly dividing the initial dataset into seventy-percent training sets and thirty-percent testing sets. Then, in order to remove any outliers and bring the data into a range of [0, 1], normalization was applied to both sets. The model development process was carried out solely on the training set, while the prediction models were tested on the testing set, which contained unseen data.

Two ANN models were developed to predict the Nmax of CFST columns: one for rectangular columns and the other for circular columns. The Nmax values from the database were the goals, and the Nmax values that the models projected were the outputs. Two ANN models were developed to predict the maximum value of the rectangular and circular columns. The models' targets were the maximum value database values, and the outputs were the maximum values that the models predicted. The following formula, which was developed and used to forecast the trend of the ascending branch, was inspired by the well-known Popovics model:

$$CapNi = Nmax\left(xyy - 1 + xy\right) \quad (1)$$

10.3389/fbuil.2024.1403460

TABLE 4 Actual and predicted value for Axial Shortening.

No	Load K.N.	As M30 CC actual	Predicted	As M30 SFRC-Actual	Predicted	As M30 CC ELE actual	Predicted	As M30 SFRC ELE actual	Predicted
1	0	0	0	0	0	0	0	0	0
2	5	0.21	0.24	0.3	0.32	0.56	0.58	1.1	1.13
3	10	0.31	0.34	0.48	0.49	0.76	0.79	1.56	1.58
4	15	0.45	0.46	0.59	0.61	0.98	1.01	1.61	1.64
5	20	0.53	0.55	0.74	0.77	1.2	1.3	1.89	1.9
6	25	0.61	0.63	0.89	0.9	1.39	1.42	2.06	2.12
7	30	0.68	0.69	1.04	1.07	1.55	1.52	2.29	2.35
8	35	0.75	0.73	1.18	1.2	1.71	1.73	2.4	2.46
9	40	0.87	0.86	1.28	1.3	1.89	1.87	2.56	2.59
10	45	0.92	0.94	1.33	1.38	2.01	2.04	2.75	2.79
11	50	0.99	1.01	1.49	1.53	2.15	2.18	2.89	2.98
12	55	1.09	1.1	1.67	1.69	2.2	2.29	3.01	3.09
13	60	1.14	1.13	1.72	1.75	2.36	2.36	3.29	3.27
14	65	1.23	1.24	1.75	1.79	2.46	2.48	3.3	3.38
15	70	1.32	1.34	1.79	1.83	2.63	2.68	3.45	3.46
16	75	1.47	1.45	1.89	1.88	2.81	2.87	3.61	3.67
17	80	1.51	1.55	1.99	2.01	2.9	3.03	3.69	3.72
18	85	1.58	1.6	2.09	2.1	3.09	3.12	3.73	3.88
19	90	1.64	1.63	2.14	2.16	3.2	3.28	3.87	3.99
20	95	1.69	1.68	2.23	2.25	3.37	3.4	4.01	4.08
21	100	1.71	1.72	2.34	2.44	3.5	3.54	4.2	4.24
22	105	1.86	1.88	2.45	2.46	3.67	3.68	4.35	4.39
23	110	1.92	1.91	2.54	2.54	3.78	3.8	4.56	4.6
24	115	1.98	1.99	2.67	2.69	3.92	3.98	4.66	4.69
25	120	2.07	2.05	2.71	2.74	4.06	4.1	5.09	5.17
26	125	2.1	2.13	2.88	2.9	4.22	4.23	5.25	5.29
27	130	2.2	2.23	2.93	2.98	4.37	4.4	5.7	5.76
28	135	2.29	2.31	3.15	3.14	4.57	4.6	5.9	6.09
29	140	2.38	2.36	3.24	3.25	4.67	4.7	6.12	6.19
30	145	2.43	2.46	3.42	3.47	4.83	4.86	6.4	6.42
31	150	2.58	2.59	3.5	3.55	5.1	5.22	6.78	6.81
32	155	2.68	2.72	3.59	3.6	5.38	5.41	6.9	6.94
33	160	2.7	2.71	3.69	3.7	5.46	5.51	6.94	6.99
34	165	2.89	2.88	3.76	3.79	5.71	5,72	7.01	7.12
35	170	2.91	2.92	3.92	3.89	5.87	5.82	7.23	7.29
36	175	2.95	2.96	3.98	4.01	5.9	5.93	7.38	7.42
37	180	2.98	2.99	4.07	4.1	6.1	6.17	7.78	7.87

(Continued on following page)

TABLE 4 (*Continued*) Actual and predicted value for Axial Shortening.

No	Load K.N.	As M30 CC actual	Predicted	As M30 SFRC-Actual	Predicted	As M30 CC ELE actual	Predicted	As M30 SFRC ELE actual	Predicted
38	185	3.09	3.1	4.25	4.26	6.28	6.32	8.1	8.2
39	190	3.18	3.2	4.38	4.38	6.34	6.37	8.56	8.81
40	195	3.21	3.23	4.41	4.45	6.67	6.78	8.9	8.91
41	200	3.32	3.34	4.56	4.51	6.75	6.81	8.94	8.97

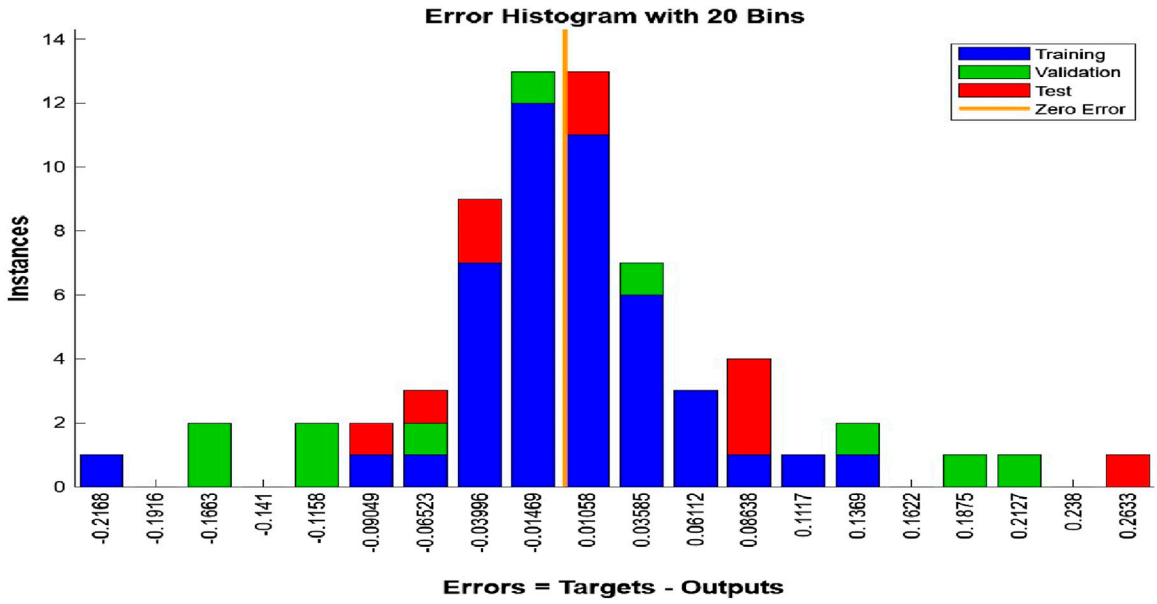

FIGURE 9
Displays the samples from the E.R. and ANN models.

X is a variable such that x = i/max, and Ni and i stand for the axial load and axial shortening at level I, respectively. The formula demonstrates that the only unknown variable is y. Trial and error was used to calculate the value of y. Eq. 1 was used to simulate the ascending branches of the 967-axial load-shortening curves in the database. The value of y for each simulation that most closely mirrored the original curve was noted. The best-fit model was created using the value of y = 3.80, as shown in Figure 5. The data from the circular and rectangular CFST columns were used to train the ANN models since the expected values of y were the goals, and the values of y were the outputs. The descending branch's trend was ascertained using Binici's model and the following equation:

$$Ni = Nre + (Nmax - Nre)\,exp\left[-\left(\Delta i - \Delta max\,\beta\right)\alpha\right] \quad (2)$$

where constants are present. Using Eq. 2, the 967 axial-shortening curves from the database were reconstructed. The procedure to compute the y value was also used to derive the values. An example where the best-fit model was developed using = 2.20 is shown in Figure 6. The simulation results, experimental data, and F.E.M. data were all determined to be best fit by values of 1.3 and 0.7 Nmax, respectively. The ANN models were trained using the data from rectangular CFST columns since the targets were the values and the outputs were the expected values. The flow diagram for the axial load-shortening curve utilizing the ANN approach is shown in Figure 7.

5.2 Performance of well-trained networks

Table 1 lists the statistical ANN model indicators that apply to all datasets (i.e., 100% of the data). The near-unity RMSE and R2 values exhibit the exceptional performance of the trained networks, which is supported by all statistical measurements. The MAPE results show a little discrepancy between the expected and actual values. Table 2 displays the statistical indicators for the training and testing sets, encompassing 80% and 20% of the data about the Artificial Neural Network (ANN) models. Notably, the statistical metrics for both the training and testing sets show remarkable consistency, suggesting that the ANN models were not subjected to overtraining. Figure 8 shows the error range (E.R.), the percentage difference between the actual and projected values for the trained models. The precision of the Artificial Neural

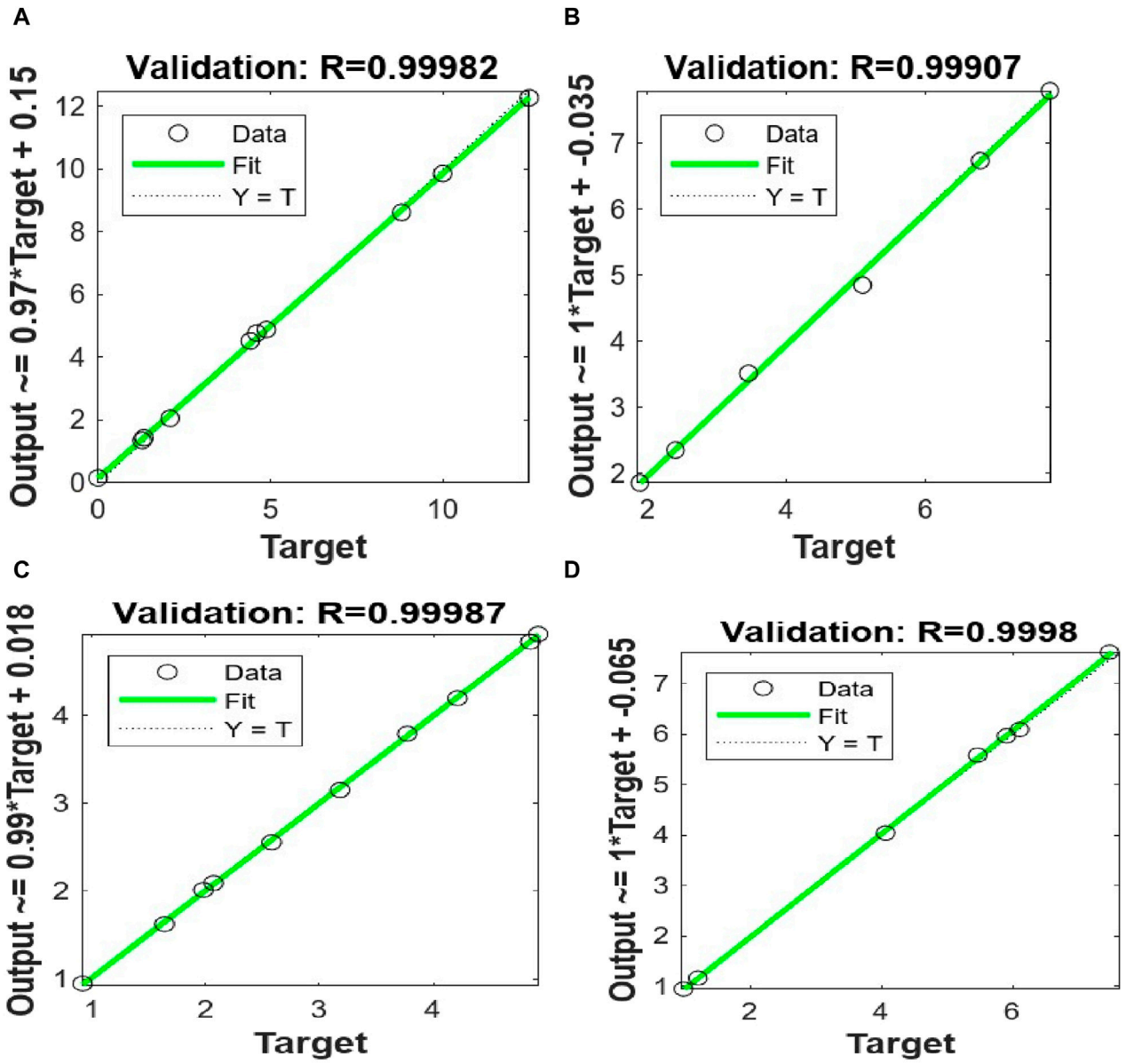

FIGURE 10
Show the validation of the model with R-values.

Network (ANN) models in forecasting target values is strikingly evident, as a substantial majority of prediction outcomes exhibit an Error Ratio (E.R.) of less than or equal to 5%. Only a minor fraction of predictions demonstrate an E.R. exceeding 5%. For instance, the E.R. was up to 5%, 4% was between 5% and 10%, and 1% was greater than 10 in 95% of the Nmax forecasts for circular columns. For instance, the experimental observation and predicted curves agreed well for the CR4-D-4-1 and CS1-1 specimens. As was already established, various researchers may report different results for the same specimen due to testing settings and configuration changes. The values of and CoV that correspond to the ultimate strengths of 12 specimens and the actual and projected strengths have a significant correlation. They were 1.01 and 0.04, respectively.

The provided data appears to be related to load testing for different parameters associated with M30 concrete, including axial shortening, actual *versus* predicted results, and the comparison of conventional concrete (CC) and steel fibre-reinforced concrete (SFRC) for both structural and environmental loading (E.L.E.) shows in Table 4. These measurements and predictions are crucial for assessing the performance and integrity of M30 concrete in various conditions and are essential for quality control and structural design purposes.

These visuals exhibit samples obtained from the Empirical Risk (E.R.) and the Artificial Neural Network (ANN) models. The comparison of these samples is essential for assessing the performance and predictive capabilities of both models. Figure 9 provides a valuable means of evaluating how well the ANN model approximates the outcomes of the E.R. model, enabling researchers and stakeholders to make informed decisions based on the model's predictive accuracy and potential applications.

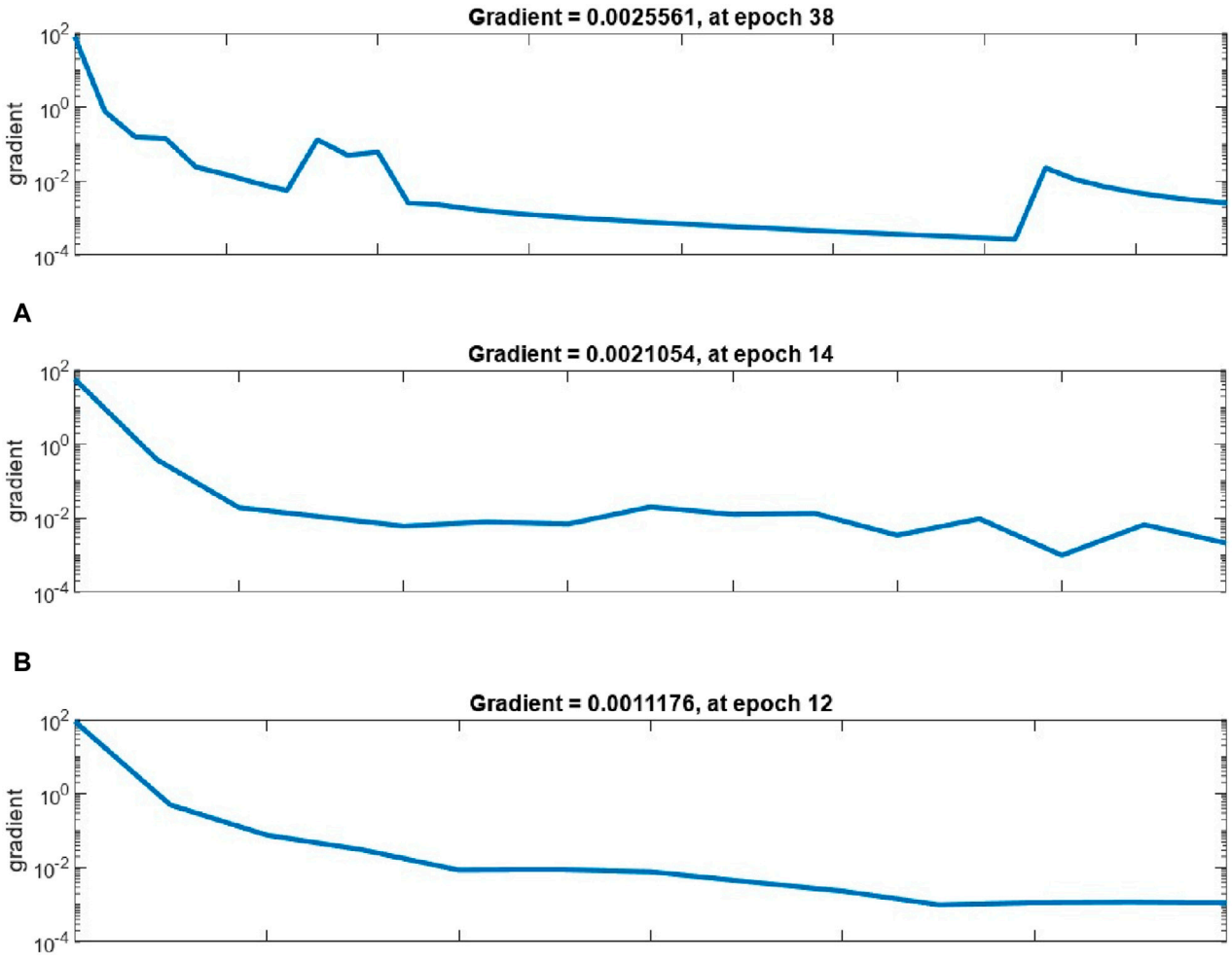

FIGURE 11
Gradient of the model.

The graphic presents the validation of the model by showcasing a series of R-values, which are statistical indicators used to assess the goodness of fit between the model's predictions and observed data. Figure 10 is a valuable visual tool for evaluating the accuracy and reliability of the model's predictions, with higher R-values indicating a more robust correlation and better fit between the model's output and real-world data.

The graphical representation provides a visual depiction of the model's gradient, revealing the rate of change of a specific parameter or function. The gradient is crucial in understanding how the model responds to variations in input variables, making Figure 11 an essential visual aid for interpreting the model's behavior and optimizing its performance.

5.3 Taylor diagram

Further, these statistical results were validated using Taylor diagram. Taylor diagrams (Kumar et al., 2023) provide a concise visual representation to evaluate the performance of different simulation models by comparing predicted and observed values. On a two-dimensional graph, it include regression coefficients, standard deviations, and root-mean-square (RMS) differences. The standard deviation is shown by the radial distance from the center, and the correlation coefficient is represented by the azimuthal angle. The RMS error is scaled to the difference between actual and projected standard deviations. The model closest to the reference point indicates the best prediction accuracy. The Taylor diagrams for the four predictions are shown in Figure 12. As can be observed, the marker location for all four predictions model is closer to the "Ref" point, validating the statistical results. The Taylor diagrams illustrate the positions of the four prediction models relative to the "Ref" point. It is evident that all four models are located closer to the "Ref" point, but the position of AS M30 CC is exactly overlapping the reference point. Thus, it can be concluded that all models prediction was good but the prediction of ANN model for AS M30 CC outperformed the other three models and obtained the best results.

5.4 Accuracy matrix

An accuracy heatmap matrix was created using the performance metrics and results of all the proposed models to show how effective

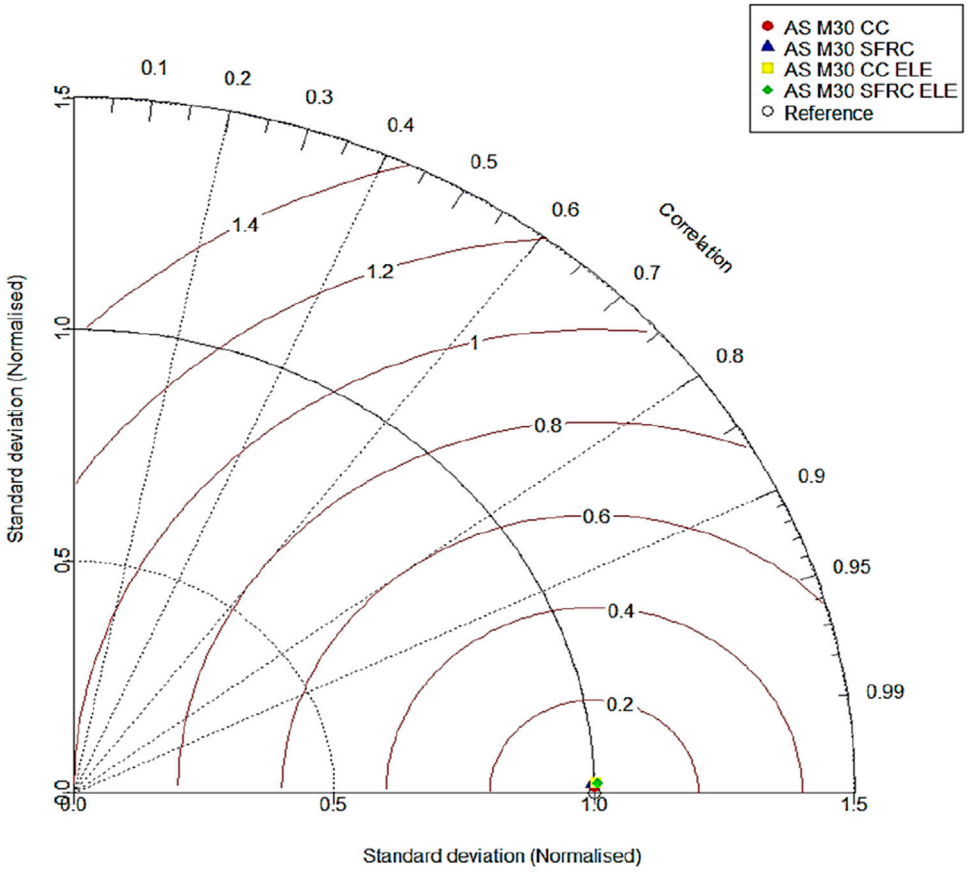

FIGURE 12
Taylor diagram for prediction models.

they were. Figure 13 shows the accuracy heatmap matrix, which represents the total accuracy of the built models. In order to thoroughly assess the effectiveness and dependability of the ANN models, a number of performance metrics, including R^2, MAE, RMSE, VAF, RSR, LMI, WMAPE, NS, WI, and PI, were carefully calculated and accuracy of these parameters is shown in Figure 13 (Isleem et al., 2023; Kumar et al., 2024). These performance parameters are derived and expressed in explicit terms in Eqs 3 through 12, where k represents the total number of observations for each parameter and q the total number of inputs used to generate the prediction. To be more precise, the variables $\hat{x}_i$ and x_i represent the predicted and actual output, respectively, and x_{mean} represents the mean value obtained from the input variables. The achieved accuracies for each performance metric were calculated using the ideal value as a benchmark. For instance, we show that $R^2 = 1$ and RMSE = 0 are the ideal values.

$$R^2 = \frac{\sum_{i=1}^{k}(x_i - x_{mean})^2 - \sum_{i=1}^{k}(x_i - \hat{x}_i)^2}{\sum_{i=1}^{k}(x_i - x_{mean})^2} \tag{3}$$

$$RMSE = \sqrt{\frac{1}{k}\sum_{i=1}^{k}(x_i - \hat{x}_i)^2} \tag{4}$$

$$VAF = 1 - \frac{var(x_i - \hat{x}_i)}{var(x_i)} \times 100\% \tag{5}$$

$$PI = adj.R^2 + 0.01VAF - RMSE \tag{6}$$

$$\text{RSR} = \frac{RMSE}{\sqrt{\left[\frac{1}{k}\sum_{i=1}^{k}(x_i - x_{mean})^2\right]}} \tag{7}$$

$$MAE = \frac{1}{k}\sum_{i=1}^{k}|(\hat{x}_i - x_i)| \tag{8}$$

$$LMI = 1 - \left[\frac{\sum_{i=1}^{k}|x_i - \hat{x}_i|}{\sum_{i=1}^{k}|x_i - x_{mean}|}\right], 0 < LMI \leq 1 \tag{9}$$

$$\text{WI} = 1 - \left[\frac{\sum_{i=1}^{k}(x_i - \hat{x}_i)^2}{\sum_{i=1}^{k}(|\hat{x}_i - x_{mean}| + |x_i - x_{mean}|)^2}\right] \tag{10}$$

$$\text{NS} = 1 - \frac{\sum_{i=1}^{k}(x_i - \hat{x}_i)^2}{\sum_{i=1}^{n}(x_i - x_{mean})^2} \tag{11}$$

$$\text{WMAPE} = \frac{\sum_{i=1}^{k}\left|\frac{x_i - \hat{x}_i}{x_i}\right| \times x_i}{\sum_{i=1}^{k} x_i}, \tag{12}$$

It can be observed in Figure 13, the predictive accuracy of ANN model for AS M30 CC is very good as the accuracy for most of the performance parameters are 100%. After ANN model for AS M30, the second best accuracy was observed for AS M30 SFRC, and AS M30 SFRC ELE prediction's accuracy was least compared to other three models. Statistical results from predictions and the Taylor's diagram validate the overall accuracy of the proposed models, which is very good shown in Figure 13.

10.3389/fbuil.2024.1403460

FIGURE 13
Accuracy matrix for prediction models.

6 Conclusion

The stated objective was examined by gathering datasets and data analysis to compare the outcomes of the developed ANN model with regressions to those of current ANN models in the construction industry. Compared to the ANN, up to 40% of the R2 values are above 0.95; however, after the 60% size, the values gradually declined below 0.95. Sizes with a 0.95 ratio will perform better and range between 40% and 60%.

According to the L.R. model, the axial load R2 value was 0.89, and the axial shortening R2 value was 0.88. The load and axial shortening regression coefficients were 0.95 in the ANN investigation. Due to its greater precision, the ANN model produced a correlation coefficient near 1. The suggested ANN model successfully predicted the axial shortening for the CFST-Column CFST SFRC. It contains the width (B), height (H), length (L/Le), diameter (d), and thickness (t), among other dimensions of rectangular steel tube columns. The accuracy of the proposed ANN model was verified. The model becomes more accurate and stable, which makes it beneficial for future studies and inquiries.

The axial shortening for the CFST-Column, or CFST SFRC, which comprises different geometries of rectangular steel tube columns, along with other measurements, has width (B), height (H), length (L/Le), diameter (d), and thickness (t)., was effectively predicted by the suggested ANN model. The accuracy of the proposed ANN model was verified. The model becomes more accurate and stable, which makes it beneficial for future studies and inquiries. For the AS M30 CC case, the ANN model showed the highest predictive accuracy; however, for the AS M30 SFRC ELE, it performed relatively worse. The Taylor diagram and accuracy matrix supported this observation and further supported the statistical conclusions. These findings highlight the ANN model's effectiveness in forecasting the behavior of Concrete-filled Steel Tubular (CFST) columns under various circumstances, providing insightful information for further study and useful applications in structural engineering.

7 Limitations and future work

This study presents a novel method for predicting the structural performance of steel tube columns filled with concrete enhanced with SFRC in the event of a fire. The goal is to investigate whether ANN can be used to simulate the properties of steel tube columns filled with SFRC-enhanced concrete and aid in their design. Obviously, the input variables chosen at this stage of the research are somewhat limited. The input parameters can be raised in the future with more experimental data, producing a simulation that is even more accurate. The accuracy of the ANN model is significantly limited by the study's reliance on a small dataset. Therefore, in order to improve the model's predictions' robustness and generalizability, future work must concentrate on increasing the dataset size and number of input parameters. Furthermore, applying sophisticated optimization algorithms like genetic algorithms or particle swarm optimization is crucial to improving the accuracy of the model because of the inherent difficulties in training ANN models with

little data. Even with limited datasets, these optimization techniques can help improve the model's performance by fine-tuning its architecture and parameters. Future iterations of the model can enhance accuracy and overcome the constraints posed by small datasets by integrating these approaches into the ANN framework. Further avenues for improving predictive accuracy and reliability in the context of CFST column behavior prediction could be found by investigating ensemble learning approaches or hybrid models that combine ANN with other machine learning techniques. Therefore, in order to maximize the performance of the ANN model and address the issues presented by small dataset sizes, future research projects should give priority to the implementation of sophisticated optimization algorithms.

Data availability statement

The original contributions presented in the study are included in the article/supplementary material, further inquiries can be directed to the corresponding authors.

Author contributions

CG: Conceptualization, Data curation, Investigation, Methodology, Software, Visualization, Writing–original draft. EZ: Data curation, Formal Analysis, Methodology, Writing–review and editing. MP: Investigation, Methodology, Resources, Supervision, Writing–original draft. SSe: Data curation, Investigation, Methodology, Project administration, Resources, Writing–review and editing. MC: Formal Analysis, Investigation, Methodology, Validation, Writing–review and editing. RK: Investigation, Project administration, Resources, Supervision, Writing–review and editing. AS: Investigation, Visualization, Writing–original draft, Writing–review and editing. SSa: Data curation, Investigation, Methodology, Visualization, Writing–review and editing. KO: Conceptualization, Data curation, Formal Analysis, Methodology, Software, Supervision, Validation, Visualization, Writing–original draft, Writing–review and editing.

Funding

The author(s) declare that no financial support was received for the research, authorship, and/or publication of this article.

Conflict of interest

The authors declare that the research was conducted in the absence of any commercial or financial relationships that could be construed as a potential conflict of interest.

Publisher's note

All claims expressed in this article are solely those of the authors and do not necessarily represent those of their affiliated organizations, or those of the publisher, the editors and the reviewers. Any product that may be evaluated in this article, or claim that may be made by its manufacturer, is not guaranteed or endorsed by the publisher.

References

Asteris, P. G., Lemonis, M. E., Le, T. T., and Tsavdaridis, K. D. (2021). Evaluation of the ultimate eccentric load of rectangular CFSTs using advanced neural network modeling. *Eng. Struct.* 248, 113297. doi:10.1016/j.engstruct.2021.113297

Chandramouli, P., Jayaseelan, R., Pandulu, G., Kumar, V. S., Murali, G., and Vatin, N. I. (2022). Estimating the axial compression capacity of concrete-filled double-skin tubular columns with metallic and non-metallic composite materials. *Materials* 15 (10), 3567. doi:10.3390/ma15103567

Đorđević, F., and Kostić, S. M. (2023). Practical ANN prediction models for the axial capacity of square CFST columns. *J. Big Data* 10 (1), 67. doi:10.1186/s40537-023-00739-y

Du, Y., Chen, Z., and Xiong, M. X. (2016). Experimental behavior and design method of rectangular concrete-filled tubular columns using Q460 high-strength steel. *Constr. Build. Mater.* 125, 856–872. doi:10.1016/j.conbuildmat.2016.08.057

Fischer, E. C., Varma, A. H., and Gordon, J. A. (2022). Performance-based structural fire engineering of steel building structures: traveling fires. *Front. Built Environ.* 8. doi:10.3389/fbuil.2022.907237

George, C., and Selvan, S. S. (2024). Integrated analysis of light gauge steel beam sections enhanced by steel fiber reinforced concrete: a comprehensive study on structural and thermal performance. *Matéria (Rio de Janeiro)* 29 (2). doi:10.1590/1517-7076-rmat-2023-0329

George, C., Senthil Selvan, S., Sathish Kumar, V., Murali, G., Giri, J., Makki, E., et al. (2024). Enhancing the fire-resistant performance of concrete-filled steel tube columns with steel fiber-reinforced concrete. *Case Stud. Constr. Mater.* 20, e02741. doi:10.1016/j.cscm.2023.e02741

Han, L.-H., Ma, D.-Y., and Zhou, K. (2018). Concrete-encased CFST structures: behaviour and application. doi:10.4995/asccs2018.2018.7109

Han, L. H., Yao, G. H., and Tao, Z. (2007). Performance of concrete-filled thin-walled steel tubes under pure torsion. *Thin-Walled Struct.* 45 (1), 24–36. doi:10.1016/j.tws.2007.01.008

Han, L. H., Yao, G. H., and Zhao, X. L. (2005). Tests and calculations for hollow structural steel (HSS) stub columns filled with self-consolidating concrete (SCC). *J. Constr. Steel Res.* 61 (9), 1241–1269. doi:10.1016/j.jcsr.2005.01.004

Hu, H.-T., Huang, C.-S., Wu, M.-H., and Wu, Y.-M. (2003). Nonlinear analysis of axially loaded concrete-filled tube columns with confinement effect. *J. Struct. Eng.* 129 (10), 1322–1329. doi:10.1061/(ASCE)0733-9445(2003)129:10(1322)

Isleem, H. F., Zewudie, B. B., Bahrami, A., Kumar, R., Xingchong, W., and Samui, P. (2023). Parametric investigation of rectangular CFRP confined concrete columns reinforced by inner elliptical steel tubes using finite element and machine learning models. *Heliyon* 10, e23666. doi:10.1016/j.heliyon.2023.e23666

Ivakhnenko, A. G. (1971). Polynomial theory of complex systems. *IEEE Trans. Syst. MAN, Cybern.* 1 (Issue 4), 364–378. doi:10.1109/tsmc.1971.4308320

Kumar, R., Rai, B., and Samui, P. (2023). Machine learning techniques for prediction of failure loads and fracture characteristics of high and ultra-high strength concrete beams. *Innov. Infrastruct. Solutions* 8, 219. doi:10.1007/s41062-023-01191-w

Kumar, R., Samui, P., and Rai, B. (2024). Prediction of the splitting tensile strength of manufactured sand based high-performance concrete using explainable machine learning. *Iran. J. Sci. Technol. Trans. Civ. Eng.* doi:10.1007/s40996-024-01401-0

Le, T.-T., Asteris, P., and Lemonis, M. (2021). Prediction of axial load capacity of rectangular concrete-filled steel tube columns using machine learning techniques. *Eng. Comput.* 38, 3283–3316. doi:10.1007/s00366-021-01461-0

Liao, J., Asteris, P. G., Cavaleri, L., Mohammed, A. S., Lemonis, M. E., Tsoukalas, M. Z., et al. (2021). Novel fuzzy-based optimization approaches for the prediction of ultimate axial load of circular concrete-filled steel tubes. *Buildings* 11 (12), 629. doi:10.3390/buildings11120629

Liew, J. Y. R., Xiong, M., and Xiong, D. (2016). Design of concrete filled tubular beam-columns with high strength steel and concrete. *Structures* 8, 213–226. doi:10.1016/j.istruc.2016.05.005

Meng, F., Zhu, M., Clifton, G., Ukanwa, K., and Lim, J. (2020). Performance of square steel-reinforced concrete-filled steel tubular columns subject to non-uniform fire. *J. Constr. Steel Res.* 166, 105909. doi:10.1016/j.jcsr.2019.105909

Mohammed, S. A., Shakor, P., S, S., Rauniyar, A., Krishnaraj, L., Kumar Singh, A., et al. (2023). An environmental sustainability roadmap for partially substituting agricultural waste for sand in cement blocks. *Front. Built Environ.* 9. doi:10.3389/fbuil.2023.1214788

Moliner, V., Espinos, A., Romero, M. L., and Hospitaler, A. (2013). Fire behavior of eccentrically loaded slender high strength concrete-filled tubular columns. *J. Constr. Steel Res.* 83, 137–146. doi:10.1016/j.jcsr.2013.01.011

Murali, G., and Azab, M. (2023). Recent research in utilization of phosphogypsum as building materials: review. *J. Mater. Res. Technol.* 25, 960–987. doi:10.1016/j.jmrt.2023.05.272

Raja, M. N. A., Shukla, S. K., and Khan, M. U. A. (2021). An intelligent approach for predicting the strength of geosynthetic-reinforced subgrade soil. *Int. J. Pavement Eng.* 23, 3505–3521. doi:10.1080/10298436.2021.1904237

Romero, M. L., Moliner, V., Espinos, A., Ibañez, C., and Hospitaler, A. (2011). Fire behavior of axially loaded slender high strength concrete-filled tubular columns. *J. Constr. Steel Res.* 67 (12), 1953–1965. doi:10.1016/j.jcsr.2011.06.012

Sakino, K., Nakahara, H., Morino, S., and Nishiyama, I. (2004). Behavior of centrally loaded concrete-filled steel-tube short columns. *J. Struct. Eng.* 130 (2), 180–188. doi:10.1061/(ASCE)0733-9445(2004)130:2(180)

Sarkar, S., Chakraborty, S., and Nayak, S. (2023). ANN-based axial strength prediction of short columns with double and bar-reinforced concrete-filled steel tubes subjected to concentric and eccentric loading. *Arabian J. Sci. Eng.* 49, 4947–4968. doi:10.1007/s13369-023-08285-8

Sathvik, S., Edwin, A., Basnett, A., Sharma, P., and Carmicheal, J. (2019a). Experiment of partial replacement of egg shell powder and coconut fibre in concrete. *Int. J. Innovative Technol. Explor. Eng.* 8 (6 Special Issue 4), 1034–1038. doi:10.35940/ijitee.F1213.0486S419

Sathvik, S., Shakor, P., Hasan, S., Awuzie, B. O., Singh, A. K., Rauniyar, A., et al. (2023). Evaluating the potential of geopolymer concrete as a sustainable alternative for thin white-topping pavement. *Front. Mater.* 10. doi:10.3389/fmats.2023.1181474

Sathvik, S., Suchith, S., Edwin, A., Jemimahcarmicheal, M., and Sheela, V. (2019b). Partial replacement of biomedical waste ASH in concrete. *Int. J. Innovative Technol. Explor. Eng.* 8 (6 Special Issue 4), 854–857. doi:10.35940/ijitee.F1172.0486S419

Sharma, P., Sathvik, S., Prasath Kumar, V. R., and Krishnaraj, L. (2022). Experimental study on properties of fresh and hardened concrete with treated waste domestic water. *Lect. Notes Civ. Eng.* 194, 123–134. doi:10.1007/978-981-16-6403-8_11

Singh, A. K., Sathvik, S. C., Krishnaraj, L., Irfan, M., Kumar, V. R. P., and Işik, C. (2023). Assessing thermo-physical products' efficiency in the building and construction industry: a bibliometric analysis approach. *Environ. Sci. Pollut. Res.* 30 (7), 16867–16877. doi:10.1007/s11356-022-25103-0

Song, T.-Y., Tao, Z., Han, L.-H., and Uy, B. (2017). Bond behavior of concrete-filled steel tubes at elevated temperatures. *J. Struct. Eng.* 143 (11). doi:10.1061/(asce)st.1943-541x.0001890

Ujwal, M. S., Kumar, G. S., Sathvik, S., and Ramaraju, H. K. (2024). Effect of soft story conditions on the seismic performance of tall concrete structures. *Asian J. Civ. Eng.* doi:10.1007/s42107-023-00968-9

Wróblewska, J., and Kowalski, R. (2020). Assessing concrete strength in fire-damaged structures. *Constr. Build. Mater.* 254, 119122. doi:10.1016/j.conbuildmat.2020.119122

Zarringol, M., and Thai, H. T. (2022). Prediction of the load-shortening curve of CFST columns using ANN-based models. *J. Build. Eng.* 51, 104279. doi:10.1016/j.jobe.2022.104279

Zhou, X., and Liu, J. (2019). Application of steel-tubed concrete structuresin high-rise buildings. *Int. J. High-Rise Build.* 8 (3), 161–167. doi:10.21022/IJHRB.2019.8.3.161